



Design of inhibitors of thymidylate kinase from *Variola virus* as new selective drugs against smallpox: part II

Danielle Rodrigues Garcia^a, Felipe Rodrigues de Souza^a, Ana Paula Guimarães^b, Teodorico Castro Ramalho^{c,d} , Alcino Palermo de Aguiar^e and Tanos Celmar Costa França^{a,d} 

^aLaboratory of Molecular Modeling Applied to Chemical and Biological Defense, Military Institute of Engineering, Rio de Janeiro, RJ, Brazil;

^bDepartment of Chemistry, Federal University of Viçosa, Viçosa, MG, Brazil; ^cLaboratory of Computational Chemistry, Department of Chemistry, UFLA, Lavras, MG, Brazil; ^dFaculty of Informatics and Management, Center for Basic and Applied Research, University of Hradec Králové, Hradec Králové, Czech Republic; ^eLaboratory of Organic Synthesis, Military Institute of Engineering, Rio de Janeiro, RJ, Brazil

Communicated by Ramaswamy H. Sarma

ABSTRACT

Acknowledging the importance of studies toward the development of measures against terrorism and bioterrorism, this study aims to contribute to the design of new prototypes of potential drugs against smallpox. Based on a former study, nine synthetic feasible prototypes of selective inhibitors for thymidylate kinase from *Variola virus* (*Var*TMPK) were designed and submitted to molecular docking, molecular dynamics simulations and binding energy calculations. The compounds are simplifications of two more complex scaffolds, with a guanine connected to an amide or alcohol through a spacer containing ether and/or amide groups, formerly suggested as promising for the design of selective inhibitors of *Var*TMPK. Our study showed that, despite the structural simplifications, the compounds presented effective energy values in interactions with *Var*TMPK and *Hss*TMPK and that the guanine could be replaced by a simpler imidazole ring linked to a $-NH_2$ group, without compromising the affinity for *Var*TMPK. It was also observed that a positive charge in the imidazole ring is important for the selectivity toward *Var*TMPK and that an amide group in the spacer does not contribute to selectivity. Finally, prototype 3 was pointed as the most promising to be synthesized and experimentally evaluated.

ARTICLE HISTORY

Received 22 August 2018
Accepted 26 November 2018

KEYWORDS

Drug design; *Variola virus*; thymidylate kinase; smallpox; docking; molecular dynamics simulations

Introduction

Chemical and biological weapons can be defined as warfare agents belonging to the class of unconventional weapons, which comprises substances or organisms of complex identification and control, which can be produced in more economically viable production systems than those of conventional weapons (Taylor & Junior, 1992). Generally speaking, these warfare agents are feared throughout the world due to their high lethality, causing panic and emotional instability in superior levels when compared to the psychological impact of conventional weapons (Bismuth, Borron, Baud, & Barriot, 2004; Byrnes, King, & Junior, 2003). It is important to point out that few countries have ideal resources to resist to chemical or biological attacks today. It is under this context that studies on the field of chemical and biological defense become paramount, needing continuous development and updating, as they are the best strategy for professional training and the developing of countermeasures against such weapons (Lindler, Lebeda, & Korch, 2004).

With regard to biological warfare agents, a prominent threat is the use of viruses with high fatality rates – such as smallpox – in terrorist attacks (Chapman, Nichols, Martinez, &

Raymond, 2010; Davenport, Satchell, & Shaw-Taylor, 2018; Hammarlund et al, 2010; Kennedy, Ovsyannikova, Jacobson, & Poland, 2009). Smallpox is an infectious disease transmitted among human beings, mainly through contact with droplets containing the virus in suspension, expelled by infected individuals. It is caused by the *Variola virus*, a virus rich in DNA-type genetic material, which genus and family are, respectively, *Orthopoxvirus* and *poxviridae* (Hendrickson, Wang, Hatcher, & Lefkowitz, 2010; Liszewski et al., 2006; Sakhatsky et al., 2008). This virus replicates itself in the cytoplasm of host cells and codifies essential enzymes for the replication and transcription of the genome, such as thymidylate and thymidine kinases (TMPK and TK). Conversely, it can also be employed in the rational development of agents used in the treatment of illnesses such as cancer, functioning as a base for chemotherapies using the TMPK gene as a reference (Caillat et al., 2008).

Despite the eradication of *Variola virus* declared by the World Health Organization (WHO) in the early 1980s, the risk of a bioterrorist attack deploying smallpox in the future is recognized as real and imminent, since there is evidence that some laboratories illicitly possess strains of this biological agent (Lindler et al., 2004). Regarding immunization,

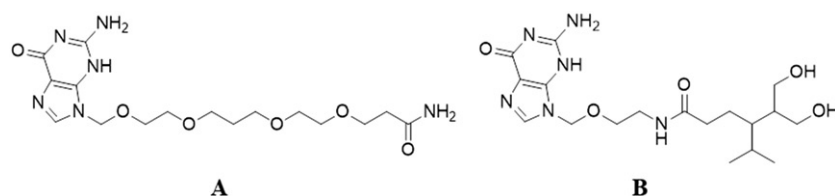


Figure 1. Selected structures proposed by Guimarães and coworkers (2015) as inhibitors for *VarTMPK*.

it should be mentioned that vaccination against smallpox was interrupted worldwide soon after its eradication in the 1980s. Besides, there are a few restrictions to its use, such as in the case of people who are HIV-positive, or have neoplasms and are under treatment with immunosuppressants. Furthermore, the side effects of the vaccine are numerous and cannot be neglected (Greenberg et al., 2013). This has motivated efforts for the development of new and more effective vaccines against smallpox (Kennedy et al., 2016; Lee, Kumar, Jhan, & Bishop, 2018; Pittman et al., 2015). However, no new and more effective vaccine is available yet.

Recently, the first drug against smallpox, tecoviramat, was approved by the FDA (U.S. Food and Drug Administration) representing a great advance, as until recently, no efficient treatment for this disease was known (Grosenbach et al., 2018; Manus, 2018). Despite encouraging, this is not enough, and the search for more drugs against this disease should continue in order to increase the therapeutic arsenal available. If we consider that almost the totality of the world population aged less than 40 is not immunized, a return of smallpox dissemination, either as a natural pandemic or in a terrorist attack, would cause catastrophic consequences. In face of this scenario, studies for developing as much as possible chemicals against molecular targets of *Variola virus* (Chaudhuri, Symons, & Deval, 2018; Chittick, Morrison, Brundage, & Nichols, 2017; Crump, Korom, Buller, & Parker, 2017; Grossi et al., 2017; Trost et al., 2015) are imperative (Damon, Damaso, & Mcfadden, 2014; Prichard, & Kern, 2012).

Recently, our research group started an innovative molecular modeling study proposing the enzyme TMPK from *Variola virus* (*VarTMPK*) as the molecular target for antivirals like cidofovir, acyclovir and its derivatives, with the aim of developing potential new inhibitors of this enzyme as drugs against smallpox (Guimarães, Ramalho, & França, 2014; Guimarães et al., 2015). Based on our first results, 10 structures were proposed and nine were highlighted as potential lead compounds for selective inhibitors of *VarTMPK*. The most promising leads pointed on these studies (Figure 1), however, are quite complex molecules, needing some structural simplifications to become more feasible from the synthetic point of view. Therefore, in order to move forward on this project, we proposed as the main objective of the present study, to minimize the structural complexity of these compounds in order to make its synthesis more viable and less costly, with a minimal impact on their potential affinity and selectivity for *VarTMPK*. For this, nine new prototypes derived from leads A and B (Figure 1) were designed and submitted to docking and molecular dynamics (MD) simulations in order to analyze their modes of interaction and, consequently, assess their selectivity within the active sites of

VarTMPK and human (*Homo sapiens sapiens*) TMPK (*HssTMPK*). Later, for the most promising results, free energy calculations were performed using the Molecular Mechanics Poisson–Boltzmann Surface Area (MM-PBSA) technique (Almeida et al., 2015; Bastos et al., 2016; Jayaram, Sprous, Young, & Beveridge, 1998; Kar, Lipowsky, & Knecht, 2013; Shao et al., 2006; Souza et al., 2017; Vorobjev, Almagro, & Hermans, 1998), a method of free energy simulation known for its high efficiency and reliability in the study of protein–ligand interactions (Wang, Greene, Xiao, Qi, & Luo, 2018).

Methodology

Investigated structures

The structures of the prototypes proposed in this study are shown in Figure 2. They are derivatives of leads A (prototypes 1–5) and B (prototypes 6–9), proposed by Guimarães et al. (2015) and shown in Figure 1. As mentioned before, these prototypes were proposed to be more feasible from the synthetic point of view, without losing the important selective interactions inside *VarTMPK* mentioned by Guimarães et al. (2015). In all cases, the guanine group was replaced by the simpler imidazole group, and the spacers were simplified to two types. The first type (in prototypes 1–5) contained only ethers, and the second type (in prototypes 6 and 7) contained one ether and one amide group. The isopropyl substituent in lead B was eliminated, since it had no relevant interaction, as reported by Guimarães et al. (2015). The guanine group on the other hand was reduced to the imidazole ring because its six-membered ring was not found by Guimarães et al. (2015) to be relevant for the selectivity related to *HssTMPK*. With the purpose of determining the predominant species of these ligands under physiologic pH (7.4), the ionization states of each one were calculated with the aid of the Chemicalize database (Swain, 2012). This software was also used to check if the leads meet the druggability criteria established by Lipinski's rule of five (Lipinski, 2004). The three-dimensional (3D) structures of the leads were constructed using the *Spartan 08® Suite* software (Shao et al., 2006), and the optimization and calculation of its atomic charges were performed employing the RM1 semi-empirical method (Gonçalves, Franca, Villar, & Pascutti, 2010; Rocha, Freire, Simas, & Stewart, 2006).

Docking studies

The structure of *VarTMPK* used in this study was the homology model compiled and validated in a previous study (Guimarães et al., 2014), while the structure of *HssTMPK* was

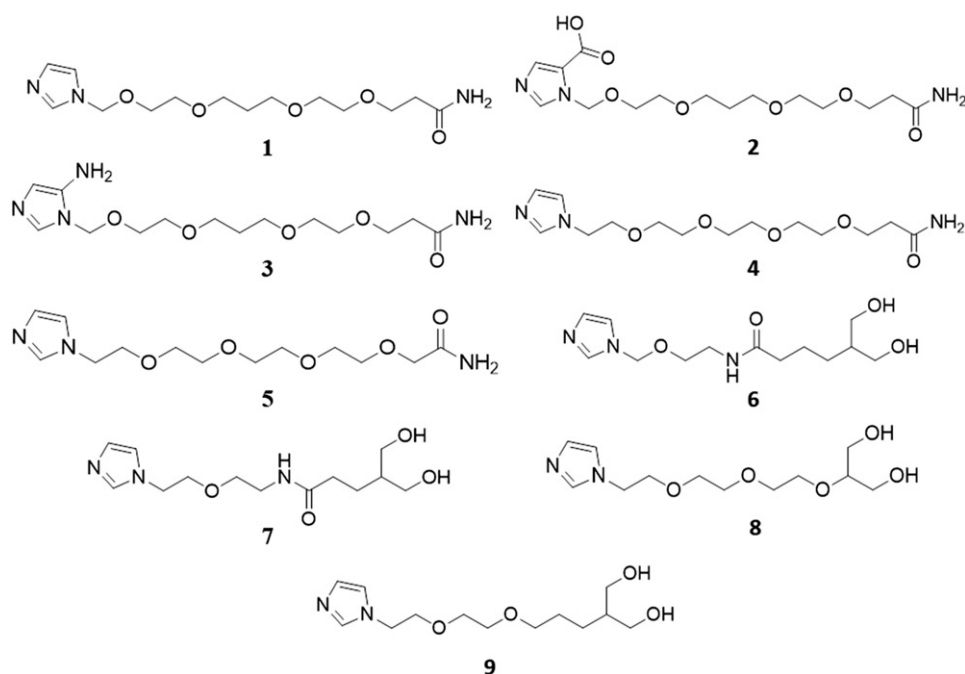


Figure 2. Structures of the proposed prototypes.

the one complexed with thymidine-5-diphosphate (TDP) and Mg^{2+} , available in the Protein Data Bank (PDB) under the code 1E2G (Berman et al., 2000). Both 3D structures of *Var*TMPK and *Hss*TMPK, were inspected and optimized before the docking studies using the software Swiss-Pdb Viewer (Guex & Peitsch, 1997) and Molegro Virtual Docker (MVD[®]) (Thomsen & Christensen, 2006).

The docking energy calculations, with the MolDock algorithm, were performed in the MVD[®] software (Thomsen & Christensen, 2006). The water molecules inside *Var*TMPK and *Hss*TMPK were maintained during the energy calculations, so that the interaction between ligands and solvents, when present, could be assessed. The validation of the docking protocol through re-docking studies was previously done by Guimarães et al. (2014). The dockings of the ligands were performed in the area where the substrate TDP and the cofactor Mg^{2+} are found. Only the Mg^{2+} was kept during docking calculations, since its interaction energies with the proposed prototypes were taken into consideration. As before (Guimarães et al., 2014), the binding sites inside *Var*TMPK and *Hss*TMPK were restricted into spheres, with radii of 6 and 10 Å for *Var*TMPK and *Hss*TMPK, respectively, around TDP, and all the residues inside these spheres were set to be flexible. The coordinates were centered on $x=8.95$, $y=22.41$ and $z=0.69$ for *Var*TMPK, and $x=13.92$, $y=75.19$ and $z=25.05$ for *Hss*TMPK.

Due to the stochastic nature of the anchoring algorithm, about 10 repetitions of the docking protocol were performed for each compound. In turn, 30 poses for the conformation and orientation of each ligand were generated for each analysis assessing the active sites of *Hss*TMPK and *Var*TMPK. The best poses for each ligand in the viral and human enzymes were selected for further MD simulations. They were chosen according to the stability of each complex formed between enzyme and ligand, the interaction energy between enzyme and cofactor, the number of hydrogen bonds observed in

each TMPK/ligand complex and the overlap between each ligand and TDP.

MD studies

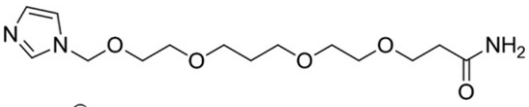
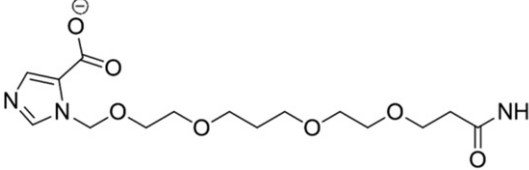
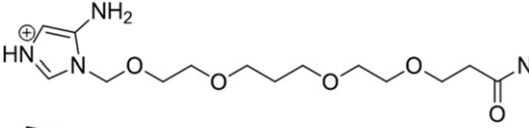
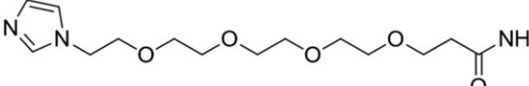
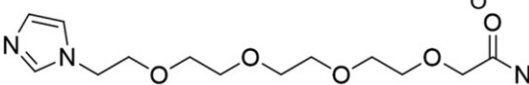
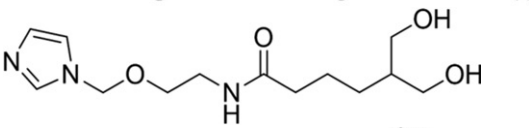
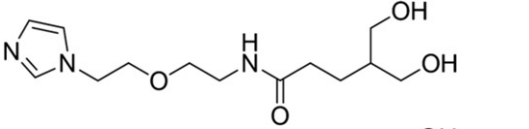
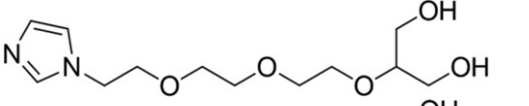
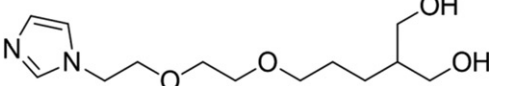
For the MD simulations, each ligand had to be parameterized (Berendsen, Van Der Spoel, & Van Drunen, 1995; Pronk et al., 2013) in order to be recognized by the OPLS-AA force field (Kaminski, Friesner, Tirado-Rives, & Jorgensen, 2001) used in this study. Thus, the parameters of topologies and coordinates were obtained using the *AnteChamber Python Parser InterfacE* (AcPype) software (Sousa da Silva, & Vranken, 2012).

The *Hss*TMPK/ligand and *Var*TMPK/ligand complexes were constructed within cubic boxes of approximately 450 nm³, containing around 13,000 Tip4P type water molecules and with periodic boundary conditions (PBCs), using the GROMACS 5.1.4 software (Abraham et al., 2015). These complexes were submitted to four steps of energy minimization, with the algorithms: (1) steepest descent with position restraint (PR) of the ligand; (2) steepest descent without PR; (3) conjugate gradients; and, lastly, (4) *quasi Newton Broyden-Fletcher-Goldfarb-Shanno* (L-BFGS) algorithm (Byrd, Lu, Nocedal, & Zhu, 1995), with a minimal energy of 1 kcal.mol⁻¹.

After the energy minimization process, the systems underwent two temperature and pressure balancing phases in order to attain equilibrium. Temperature equilibrium was reached by using the NVT ensemble (constant volume and temperature) for 100 ps, while pressure equilibrium was reached with the NPT ensemble (constant pressure and temperature), also for 100 ps. Both phases kept their particle numbers fixed.

After attaining system equilibrium, the MD simulations were performed in two stages. Firstly, the complexes were submitted to 500 ps of MD at 310 K with PR for the entire system, except for water molecules, in order to ensure the

Table 1. Molecular structures of ligands predicted through protonation analysis under physiologic pH (7.4).

Prototype	Structure ^a	% of micro species ^a	Meet the druggability criteria of the Lipinski rule? ^b
1		87.09	Yes
2		78.37	Yes
3		78.25	Yes
4		89.04	Yes
5		89.04	Yes
6		87.08	Yes
7		89.04	Yes
8		89.04	Yes
9		89.04	Yes

^aCalculated through Chemicalize web-based resource (<https://chemicalize.com/welcome>) (Swain, 2012) as the highest percentage of this micro species.

^b(Lipinski, 2004).

equilibrium of solvent molecules around the enzyme residues. Lastly, the systems were submitted to 100,000 ps of MD simulation at 310K without PR, with 2 fs of integration time, and a cutting radius of 10 Å for long-distance interactions. This study protocol was previously tested so as to ascertain that the proposed conditions would suffice for the conduction of the systems toward equilibrium. With the aim of reproducing the protonation of some residues under physiological conditions, the Glu and Asp residues were assigned with negative charges, and the Lys and Arg residues were assigned with positive charges.

The *Visual Molecular Dynamics* (VMD) software (Humphrey, Dalke, & Schulten, 1996) was used to analyze the MD results of the systems, and plots of variation of total energy, root-mean-square-deviation (RMSD) and average number of hydrogen bonds were drawn with the Origin[®] software (Edwards, 2002).

Determining free energy

The MM-PBSA method is employed to predict the free energy of binding processes, where the concepts of molecular mechanics and continuous solvent models are combined

(Evertts, Zee, & Garcia, 2010; Genheden & Ryde, 2015; Kumari, Kumar, & Lynn, 2014; Luscombe, Austin, Berman, & Thornton, 2000; Norambuena & Melo, 2010).

The study of the free energy of a system is the measure of the amount of energy usable by this system, consisting of a process by which one can indicate, for instance, whether the formation of bonds in a complex at constant temperature and pressure is spontaneous (freeing energy) or non-spontaneous (requiring energy). Because of that, this phase is extremely important for the purposes of this study, since through the average values of free binding energy, we will be able to infer which prototype is more interesting and promising in relation to the process of selectively inhibiting VarTMPK.

Lastly, the determination of the free energy of formation of the complexes, in association to the MD simulations, takes into consideration three energetic terms in its calculation of binding energy: (1) changes in the potential energy of the system in vacuum; (2) polar and apolar solvation of the different species; and (3) the entropy related to the formation of the complexes during the gaseous phase (Almeida et al., 2018; Genheden & Ryde, 2015; Kumari et al., 2014).

Table 2. Docking results for the prototypes inside the active sites of *Var*TMPK and *Hss*TMPK.

Prototype	$E_{\text{interaction}}$ (kcal.mol ⁻¹)		E_{cofactor} (kcal.mol ⁻¹)		H-bond energy (kcal.mol ⁻¹)		H-bond interactions				$\Delta E_{\text{interaction}}$ ^a (kcal.mol ⁻¹)
	<i>Var</i> TMPK	<i>Hss</i> TMPK	<i>Var</i> TMPK	<i>Hss</i> TMPK	<i>Var</i> TMPK	<i>Hss</i> TMPK	<i>Var</i> TMPK		<i>Hss</i> TMPK		
1	-151.60	-124.33	-1.03	-2.07	-13.57	-10.44	Arg41 Arg72 Tyr144	Lys14 Glu142 H ₂ O	Arg45 Arg97	Arg76 H ₂ O	27.27
2	-152.53	-116.43	-2.24	-2.86	-12.76	-11.34	Arg41 Tyr144 Arg72	Glu145 Asp13	Arg76 Ser101 Arg97	Asp15 H ₂ O	36.10
3	-123.68	-62.92	-5.60	-0.08	-8.90	-5.51	Asp13 Lys14 Arg72	Tyr94 H ₂ O	Pro43 Arg16 H ₂ O		60.76
4	-133.18	-101.31	-4.63	-3.42	-8.90	-5.51	Asp13 Lys14 Arg41	Arg72 Ser97 H ₂ O	Arg76 Ser101	Arg97 H ₂ O	31.87
5	-132.57	-110.51	-2.67	-4.97	-9.74	-11.15	Asp13 Lys14 Arg72	Tyr144 H ₂ O	Asp15 Arg97	Arg76 H ₂ O	22.06
6	-106.83	-126.01	-3.39	-1.87	-10.15	-16.26	Arg72 Asp92 Asn37	Phe38 H ₂ O	Arg76 Glu152 Asp15	Arg97 H ₂ O	-19.18
7	-120.45	-116.91	-0.71	-0.25	-16.18	-10.96	Lys14 Arg72 Glu142	Arg97 H ₂ O	Arg76 Arg45 H ₂ O		3.54
8	-118.20	-102.38	-5.26	-2.28	-12.25	-11.16	Arg72 Phe38 Arg41	Lys17 Asp13 H ₂ O	Arg76 Asp15	Arg97 H ₂ O	15.82
9	-123.47	-92.84	-2.86	-2.07	-15.51	-15.24	Arg72 Phe38 Asp92	Lys17 Asp13	Arg76 Arg16 Asp15	Arg97 H ₂ O	30.63
TDP ^b	-228.18	-195.60	-50.38	-18.13	-3.82	-13.97	Asp13 Lys17 Asn37	Arg41 Arg72 Arg93	Asp15 Arg45 Arg76	Arg97 H ₂ O	-
Prototype A ^b	-202.46	-187.77	-34.65	-40.72	-12.54	-12.94	Lys14 Lys17 Phe38	Asp92 Arg93 H ₂ O	Arg16 Lys19 Phe42 Arg76	Arg97 Ser101 H ₂ O	14.69
Prototype B ^b	-222.55	-161.09	-38.43	-27.72	-18.71	-13.16	Asp13 Lys17 Thr18 Phe38	Arg72 Asp92 Tyr94 H ₂ O	Asp15 Arg16 Lys19 Pro43	Arg45 Arg76 H ₂ O	61.46

^a $E_{\text{interaction}}(\text{VarTMPK}) - E_{\text{interaction}}(\text{HssTMPK})$.^bResults from Guimarães et al., 2015.

For all the enzyme/ligand complexes, MM-PBSA calculations were performed using the *g_mmpbsa* tool (Kumari et al., 2014) from the GROMACS package. In order to consider non-correlated frames, the structures for the free energy calculations were obtained at 500 ps each.

Results and discussion

Docking studies

Prediction of the ionization states using Chemicalize (Swain, 2012) showed that only prototypes 2 and 3 are ionized under physiologic pH, while the others are neutral. The predicted species shown in Table 1 were, then, used in the docking studies inside *Var*TMPK and *Hss*TMPK, complexed with TDP and Mg²⁺, which results are shown in Table 2. Chemicalize (Swain, 2012) results also showed that all prototypes meet the druggability criteria established by the Lipinski rule of five (Lipinski, 2004).

As can be seen in Table 2, all compounds but prototype 6 presented lower energies of interaction with *Var*TMPK, in relation to *Hss*TMPK. Besides, from the values of $\Delta E_{\text{interaction}}$ (Table 2), it is noticeable that prototypes 2, 3, 4 and 9 are

the compounds with the higher energy differences between *Var*TMPK and *Hss*TMPK. This suggests that they are the most selective compounds regarding *Var*TMPK. Therefore, these prototypes were selected for further MD studies.

It is important to mention that prototype 3 was the one with the greatest $\Delta E_{\text{interaction}}$ value (60.76 kcal.mol⁻¹) and that it also presented the lowest affinity for *Hss*TMPK, establishing hydrogen bonds only with residues Arg16 and Pro43, which are not part of the active site. This can also be related to the greater distance between the cofactor Mg²⁺ of *Hss*TMPK and the carbonyl group of prototype 3 (4.87 Å), leading to an interaction energy with the cofactor (-0.08 kcal.mol⁻¹) inferior to the one found for *Var*TMPK (-5.60 kcal.mol⁻¹). These results point to prototype 3 as the most promising selective inhibitor, based on the docking studies. The best poses obtained for prototype 3 inside *Var*TMPK and *Hss*TMPK are shown in Figure 3.

MD studies

Based on the docking results, prototypes 2, 3, 4 and 9 were selected for additional MD simulation studies with the

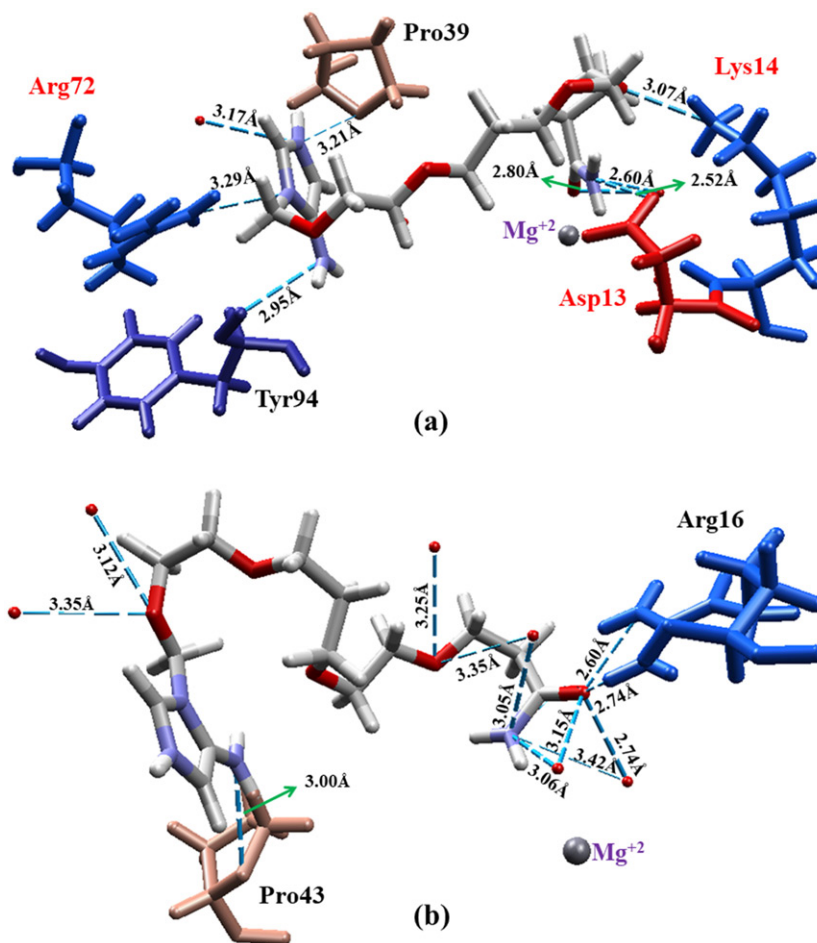


Figure 3. Best molecular docking poses for prototype 3 inside (a) *VarTMPK* and (b) *HssTMPK*. Interacting residues are shown in different colors, and residues belonging to the active site are labeled in red..

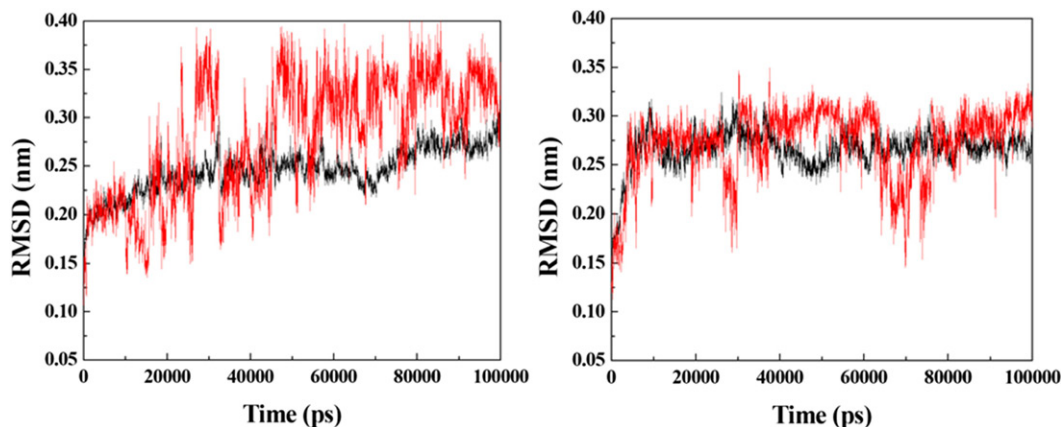


Figure 4. RMSD for the systems formed between the enzymes (in black) and prototype 2 (in red). Left: *VarTMPK*/prototype 2; right: *HssTMPK*/prototype 2.

purpose of investigating their dynamic behaviors inside *VarTMPK* and *HssTMPK*. Energy plots of the simulations (data not shown) showed stabilization before 50 ns of simulation for all the systems studied. Next, RMSD analyses were performed for each system in order to verify and compare the variations of positions of the prototypes within the active sites of *VarTMPK* and *HssTMPK* and thus to determine the most promising prototypes as selective inhibitors on the basis of their dynamical behavior. The RMSD plots obtained are shown in Figures 4–7.

As can be observed in Figure 4, the *VarTMPK*/prototype 2 and *HssTMPK*/prototype 2 complexes did not attain equilibrium during the entire simulation time. A large RMSD variation of more than 0.20 nm was observed for prototype 2, inside *VarTMPK*, since the beginning of the simulation, suggesting that this compound does not stabilize itself inside the enzyme. Regarding *HssTMPK*, the behavior of this prototype showed some stabilization during most of the simulation, but it also showed large variations around 30 ns and between 60 and 80 ns.

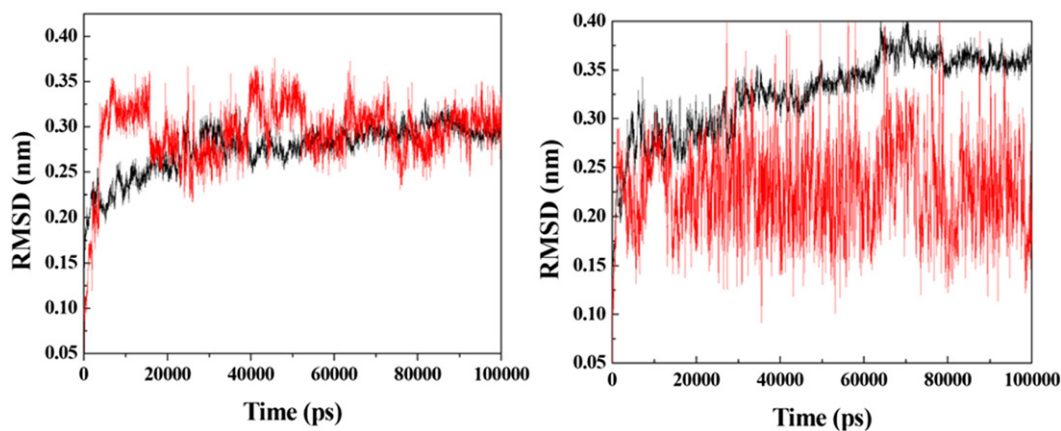


Figure 5. RMSD for the systems formed between the enzymes (in black) and prototype 3 (in red). Left: *Var*TMPK/prototype 3; right: *Hss*TMPK/prototype 3.

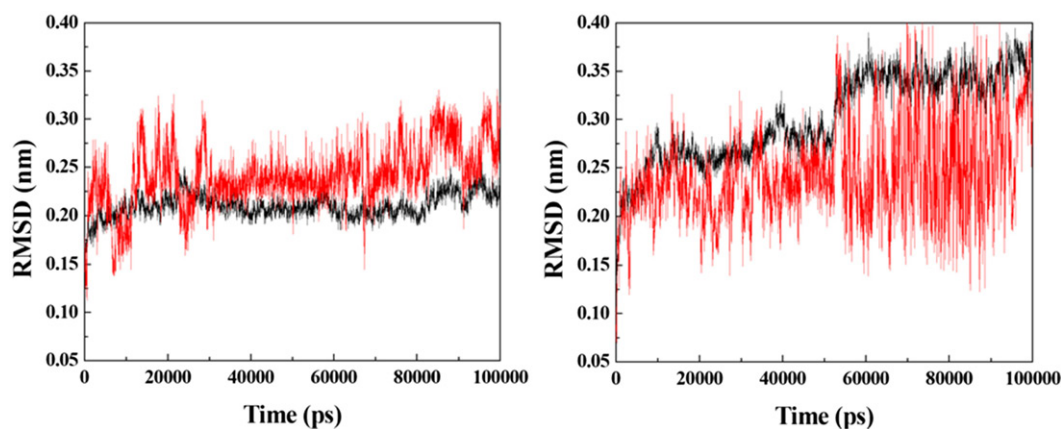


Figure 6. RMSD for the systems formed between the enzymes (in black) and prototype 4 (in red). Left: *Var*TMPK/prototype 4; right: *Hss*TMPK/prototype 4.

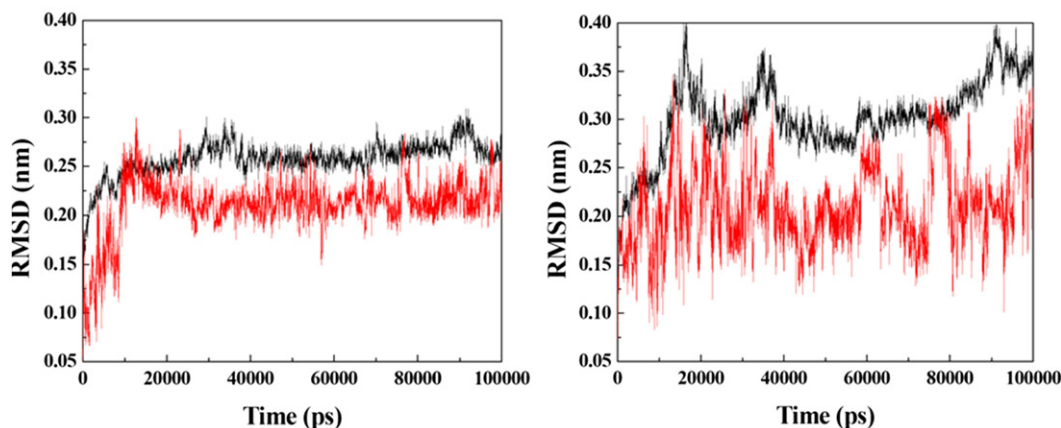


Figure 7. RMSD for the systems formed between the enzymes (in black) and prototype 9 (in red). Left: *Var*TMPK/prototype 9; right: *Hss*TMPK/prototype 9.

The RMSD plots for the *Var*TMPK/prototype 3 and *Hss*TMPK/prototype 3 complexes (Figure 5) show that, inside *Var*TMPK, this prototype presented no variation larger than 0.10 nm, tending toward stabilization after 50 ns of simulation. Inside *Hss*TMPK, on the other hand, one can see that this prototype could not achieve stability, with variations of around 0.30 nm, since the beginning of the simulation. This is indicative of the absence of stabilizing interactions inside *Hss*TMPK, suggesting some selectivity toward *Var*TMPK.

Figure 6 shows the RMSD plots for the *Var*TMPK/prototype 4 and *Hss*TMPK/prototype 4 complexes. Inside *Var*TMPK,

this prototype shows some stabilization after 30 ns of simulation, but destabilizes again after 60 ns, until the end of the simulation, with variations close to 0.15 nm. Inside *Hss*TMPK, this behavior was even more aggravated, with variations after 50 ns of around 0.25 nm, until the end of simulation. This result suggests that, despite having more affinity for *Var*TMPK, this prototype is unable to become stable inside neither of the enzymes during the simulated time.

The RMSD plots for the *Var*TMPK/prototype 9 and *Hss*TMPK/prototype 9 complexes (Figure 7) show that this prototype stabilizes itself inside *Var*TMPK, starting around

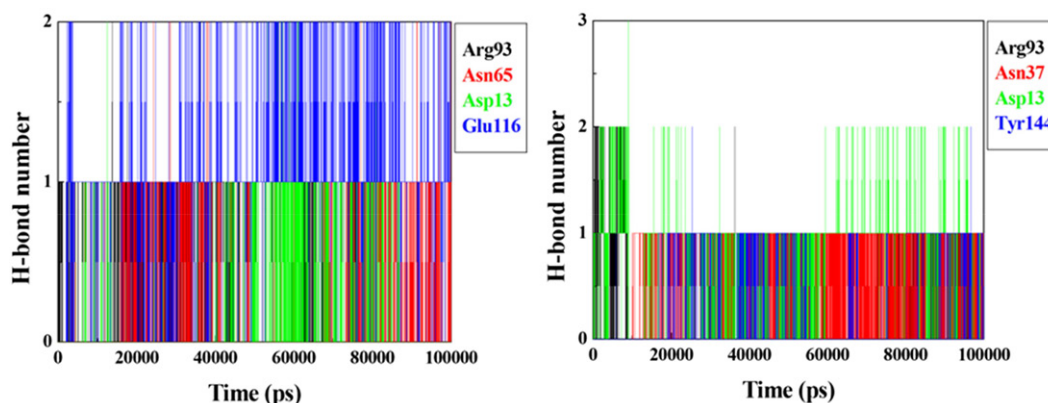


Figure 8. Plots of mean H-bonds formed by prototypes 3 (left) and 9 (right) inside *VarTMPK* during the 100 ns of MD simulation.

Table 3. MM-PBSA results for prototypes 3 and 9.

Structures	Binding energies $\text{kJ}\cdot\text{mol}^{-1}$	
	<i>VarTMPK</i>	<i>HssTMPK</i>
3	-142.22	-68.77
9	-29.16	-53.79

15 ns of simulation, with variations close to 0.05 nm until the end of the simulation, while inside *HssTMPK*, stabilization never happens, with variations of around 0.20 nm since the beginning of the simulation.

Results of the RMSD analysis suggest that, among the compounds chosen for the MD simulations, only prototypes 3 and 9 are possible inhibitors for *VarTMPK* once they were the only ones capable of stabilizing well inside the active site of the viral enzyme. These compounds also did not stabilize well inside *HssTMPK*, corroborating with the docking results pointing them as selective inhibitors. The plots of H-bonds observed for these prototypes during the 100 ns of MD simulations, shown in Figure 8, confirm the H-bond with Asp13 observed for both prototypes during the docking process. They also show additional H-bonds formed with residues Asn65, Arg93 and Glu116 for prototype 3, and with Asn37, Arg93 and Tyr144 for prototype 9. It is important to mention that Asp13, Asn65 and Arg93 are residues belonging to the active site of *VarTMPK*.

Because the MD process is the assessment of the dynamic behavior of the ligands inside a complex, i.e. an analysis involving the movement of ligand and protein structures, its results may often not corroborate the docking results. According to Chen (2015), during an MD simulation, a ligand can leave the active site of the protein, which cannot be observed in a docking study due to the movement restriction imposed by this procedure. Therefore, our docking and MD simulation results are complimentary and helps to refine the investigation on the capacity of the prototypes to selectively inhibit *VarTMPK*.

Free energy determination

Table 3 shows the results of the MM-PBSA calculations for prototypes 3 and 9 inside *VarTMPK* and *HssTMPK*. As one can see, prototype 3 presented a binding energy of $-142.22 \text{ kJ}\cdot\text{mol}^{-1}$ inside *VarTMPK* versus $-68.77 \text{ kJ}\cdot\text{mol}^{-1}$

inside *HssTMPK*, while prototype 9 presented $-29.16 \text{ kJ}\cdot\text{mol}^{-1}$ versus $-53.79 \text{ kJ}\cdot\text{mol}^{-1}$.

Figures 9 and 10 present an illustration of the favorable and unfavorable energetic contributions of some residues to the enzyme/ligand complexes for prototypes 3 and 9, respectively. Figure 9 shows that the residues that contributed to the binding energy of the *HssTMPK*/prototype 3 complex are located outside the active site of *HssTMPK*, indicating that prototype 3 did not become stable within it, remaining outside the active site.

The behavior demonstrated by each compound during the MD simulations allowed us to assess the affinity of the enzymes toward the structures; however, the calculation of the free binding energy permitted the assessment of the differences in affinity among the species integrating the complexes. The differences in interaction energy show that, very probably, the quaternary nitrogen in prototype 3 is of great importance to its affinity for the viral enzyme.

Despite the favorable MD results for the *VarTMPK*/prototype 9 complex, the binding energy calculations showed that prototype 9 did not demonstrate enough affinity toward the interaction site of the viral enzyme to remain stable, as presented in Table 3. Such instability is probably related to the fact that prototype 9 does not contain the imidazole ring on its protonated form neither the $-\text{NH}_2$ substituent in the imidazole ring, in comparison with prototype 3. The $-\text{NH}_2$ group showed in the docking studies to be able to establish H-bonds inside *VarTMPK*, while the positive charge in the imidazole ring helps the molecule to stabilize inside the more negative pocket of *VarTMPK*. The absence of these groups in the structure can hamper interactions with the amino acids in the protein, destabilizing prototype 9 inside the viral enzyme.

Conclusion

From the two selective inhibitors for *VarTMPK* proposed by Guimarães et al (2015), we were able to design structures of nine new prototypes that are much simpler from a synthetic point of view, but still able to keep effective energy values in interactions with *VarTMPK* and *HssTMPK*. Docking studies pointed to prototypes 2, 3, 4, and 9 as potential selective inhibitors of *VarTMPK*, with prototype 3 as the most promising. In the MD simulations, prototypes 3 and 9 demonstrated

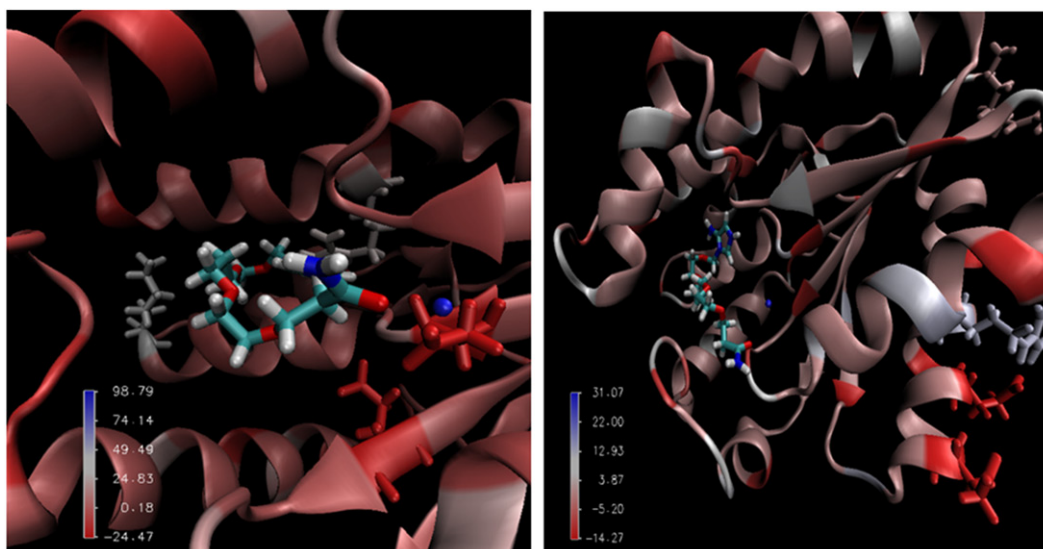


Figure 9. Main interactions of the complexes of *Var*TMPK/prototype 3 (left) and *Hss*TMPK/prototype 3 (right) calculated by MM-PBSA.

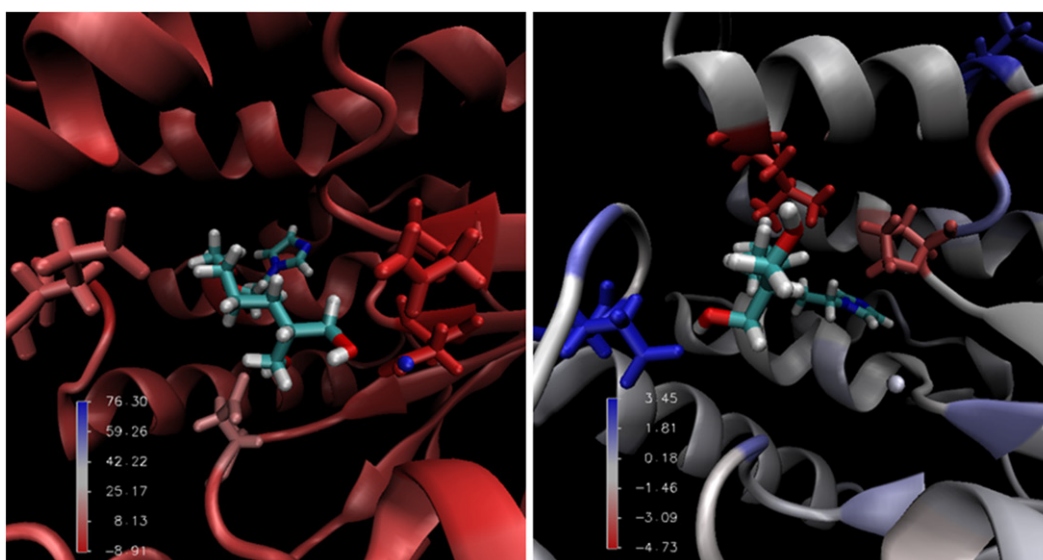


Figure 10. Main interactions of the complexes of *Var*TMPK/prototype 9 (left) and *Hss*TMPK/prototype 9 (right) calculated by MM-PBSA.

the highest stabilities inside *Var*TMPK, with the smallest RMSD variations. However, the MM-PBSA results did not corroborate prototype 9 as a selective inhibitor of *Var*TMPK. We believe that this is due to the fact that prototype 9 is neutral under physiological conditions and does not contain the $-NH_2$ substituent in the imidazole ring. This could compromise its stabilization inside *Var*TMPK. Among the structural modifications proposed on prototypes A and B from Guimarães et al. (2015), we observed that the simplification of the guanine to an imidazole ring should not compromise the affinity of the ligand for *Var*TMPK, since a H-bond donor group, like an $-NH_2$, is kept as substituent in the imidazole ring. It was also observed that a positive charge in the imidazole ring is important for the selectivity toward *Var*TMPK. However, the inclusion of an amide group in the middle or the extremity of the spacer was not observed to contribute for any selectivity. Based on our results, we believe that prototype 3 has a great potential as a selective inhibitor of *Var*TMPK and, therefore, a new drug against smallpox. In order to validate and

scale up this work, we think that it is worth synthesizing and experimentally evaluating this molecule.

Disclosure statement

No potential conflict of interest was reported by the authors.

Funding

The authors are grateful to the Brazilian agencies CNPq (grant 306156/2015-6 – T.C.C.F.) and FAPERJ (grant number 02/202.961/2017 – T.C.C.F.), for financial support and to the Military Institute of Engineering, Federal University of Lavras, Federal University of Viçosa and University of Hradec Kralové for the infrastructure. This work was also supported by the excellence FIM project.

ORCID

Teodorico Castro Ramalho  <https://orcid.org/0000-0002-7324-1353>
Tanos Celmar Costa França  <https://orcid.org/0000-0002-6048-8103>

References

- Abraham, M. J., Murtola, T., Schulz, R., Pall, S., Smith, J. C., Hess, B., & Lindahl, E. (2015). GROMACS High performance molecular simulations through multi-level parallelism from laptops to supercomputers. *Software X*, 1-2,19–25. doi:10.1016/j.softx.2015.06.001
- Almeida, J. S. D., Guizado, T. R. C., Guimarães, A. P., Ramalho, T. C., Gonçalves, A. S., Koning, M. C., & Franca, T. C. C. (2015). Docking and molecular dynamics studies of peripheral site ligand-oximes as reactivators of sarin-inhibited human acetylcholinesterase. *Journal of Biomolecular Structure and Dynamics*, 34,2632–2642. doi:10.1080/07391102.2015.1124807
- Almeida, J. S. F. D., Cavalcante, S. F. A., Dolezal, R., Kuca, K., Musilek, K., Jun, D., & Franca, T. C. C. (2018). Molecular modeling studies on the interactions of aflatoxin B1 and its metabolites with the peripheral anionic site (PAS) of human acetylcholinesterase. *Journal of Biomolecular Structure and Dynamics*, 1–8 [published online]. doi:10.1080/07391102.2018.1475259
- Bastos, L. C., Souza, F. R., Guimarães, A. P., Sirouspour, M., Guizado, T. R. C., Forgione, P., ... Franca, T. C. C. (2016). Virtual screening, docking and dynamics of potential new inhibitors of dihydrofolate reductase from *Yersinia pestis*. *Journal of Biomolecular Structure and Dynamics*, 34(10),2184–2198. 2016. doi:10.1080/07391102.2015.1110832
- Berendsen, H. J. C., Van Der Spoel, D., & Van Drunen, R. (1995). GROMACS: A message-passing parallel molecular dynamics implementation. *Computer Physics Communications*, 91(1-3),43–56. doi:10.1016/0010-4655(95)00042-E
- Berman, H. M., Westbrook, J., Feng, Z., Gilliland, G., Bhat, T. N., Weissig, H., ... Bourne, P. E. (2000). The protein data bank. *Nucleic Acids Research*, 28(1),235–242. doi:10.1093/nar/28.1.235
- Bismuth, C., Borron, S. W., Baud, F. J., & Barriot, P. (2004). Chemical weapons: Documented use and compounds on the horizon. *Toxicology Letters*, 149(1-3),11–18. doi:10.1016/j.toxlet.2003.12.016
- Byrd, R. H., Lu, P., Nocedal, J., & Zhu, C. (1995). A limited memory algorithm for bound constrained optimization. *SIAM Journal on Scientific Computing*, 16(5),1190–1208. doi:10.1137/0916069
- Byrnes, M. E., King, D. A., & Junior, P. M. T. (2003). *Nuclear, chemical, and biological terrorism: Emergency response and public protection*. Boca Raton, FL: CRC Press.
- Caillat, C., Topalis, D., Agrofoglio, L. A., Pochet, S., Balzarini, J., Deville-Bonne, D., & Meyer, P. (2008). Crystal structure of poxvirus thymidylate kinase: An unexpected dimerization has implications for antiviral therapy. *Proceedings of the National Academy of Sciences of the United States of America*, 105(44),16900–16905. doi:10.1073/pnas.0804525105
- Chapman, J. L., Nichols, D. K., Martinez, M. J., & Raymond, J. W. (2010). Animal models of orthopoxvirus infection. *Veterinary Pathology*, 47(5),852–870. doi:10.1177/0300985810378649
- Chaudhuri, S., Symons, J. A., & Deval, J. (2018). Innovation and trends in the development and approval of antiviral medicines: 1987–2017 and beyond. *Antiviral Research*, 155,76–88. doi:10.1016/j.antiviral.2018.05.005
- Chen, Y.-C. (2015). Beware of docking!. *Trends in Pharmacological Sciences*, 36(2),78–95. doi:10.1016/j.tips.2014.12.001
- Chittick, G., Morrison, M., Brundage, T., & Nichols, W. G. (2017). Short-term clinical safety profile of brincidofovir: A favorable benefit risk proposition in the treatment of smallpox. *Antiviral Research*, 143,269–277. doi:10.1016/j.antiviral.2017.01.009
- Crump, R., Korom, M., Buller, R. M., & Parker, S. (2017). Buccal viral DNA as a trigger for brincidofovir therapy in the mousepox model of smallpox. *Antiviral Research*, 139,112–116. doi:10.1016/j.antiviral.2016.12.015
- Damon, I. K., Damaso, C. R., & Mcfadden, G. (2014). Are we there yet? The smallpox research agenda using variola virus. *PLoS Pathogens*, 10,1–3. doi:10.1371/journal.ppat.1004108.
- Davenport, R. J., Satchell, M., & Shaw-Taylor, L. M. W. (2018). The geography of smallpox in England before vaccination: A conundrum resolve. *Social Science & Medicine*, 206,75–85. doi:10.1016/j.socscimed.2018.04.019
- Edwards, M. (2002). Origin 7.0: Scientific graphing and data analysis software. *Journal of Chemical Information and Computer Sciences*, 42,1270–1271. doi:10.1021/ci0255432
- Everetts, A. G., Zee, B. M., & Garcia, B. A. (2010). Modern approaches for investigating epigenetic signaling pathways. *Journal of Applied Physiology*, 109(3),927–933. doi:10.1152/jappphysiol.00007.2010
- Genheden, S., & Ryde, U. (2015). The MM/PBSA and MM/GBSA methods to estimate ligand-binding affinities. *Expert Opinion on Drug Discovery*, 10(5),449–461. doi:10.1517/17460441.2015.1032936
- Gonçalves, A. S., Franca, T. C. C., Villar, J. D. F., & Pascutti, P. G. (2010). Conformational analysis of toxogonine, TMB-4 and HI-6 using PM6 and RM1 methods. *Journal of the Brazilian Chemical Society*, 21(1),179–184. doi:10.1590/S0103-50532010000100025
- Greenberg, R. N., Overton, E. T., Haas, D. W., Frank, I., Goldman, M., von Krempelhuber, A., ... Chaplin, P. (2013). Safety, immunogenicity, and surrogate markers of clinical efficacy for modified vaccinia Ankara as a smallpox vaccine in HIV-infected subjects. *The Journal of Infectious Diseases*, 207(5),749–758. doi:10.1093/infdis/jis753
- Grosenbach, D. W., Honeychurch, K., Rose, E. A., Chinsangaram, J., Frimm, A., Maiti, B., ... Hruby, D. E. (2018). Oral tecovirimat for the treatment of smallpox. *New England Journal of Medicine*, 379(1),44–53. doi:10.1056/NEJMoa1705688
- Grossi, I. M., Foster, S. A., Gainey, M. R., Krile, R. T., Dunn, J. A., Brundage, T., & Khouri, J. M. (2017). Efficacy of delayed brincidofovir treatment against a lethal rabbitpox virus challenge in New Zealand White rabbits. *Antiviral Research*, 143,278–286. doi:10.1016/j.antiviral.2017.04.002
- Guex, N., & Peitsch, M. C. (1997). SWISS-MODEL and the Swiss-PdbViewer: An environment for comparative protein modeling. *Electrophoresis*, 18(15),2714–2723. doi:10.1002/elps.1150181505
- Guimarães, A. P., de Souza, F. R., Oliveira, A. A., Gonçalves, A. S., de Alencastro, R. B., Ramalho, T. C., & Franca, T. C. C. (2015). Design of inhibitors of thymidylate kinase from Variola virus as new selective drugs against smallpox. *European Journal of Medicinal Chemistry*, 91,72–90. doi:10.1016/j.ejmech.2014.09.099
- Guimarães, A. P., Ramalho, T. C., & Franca, T. C. C. (2014). Preventing the return of smallpox: Molecular modeling studies on thymidylate kinase from Variola virus. *Journal of Biomolecular Structure and Dynamics*, 32(10),1601–1612. doi:10.1080/07391102.2013.830578
- Hammarlund, E., Lewis, M. W., Haniff, J. M., Mori, M., Koudelka, C. W., & Slifka, M. K. (2010). Antiviral immunity following smallpox virus infection: A case-control study. *Journal of Virology*, 84(24),12754–12760. doi:10.1128/JVI.01763-10
- Hendrickson, R. C., Wang, C., Hatcher, E. L., & Lefkowitz, E. J. (2010). Orthopoxvirus genome evolution: The role of gene loss. *Viruses*, 2(9),1933–1967. doi:10.3390/v2091933
- Humphrey, W., Dalke, A., & Schulten, K. (1996). VMD: Visual molecular dynamics. *Journal of Molecular Graphics and Modelling*, 14(1),33–38. doi:10.1016/0263-7855(96)00018-5
- Jayaram, B., Sprou, D., Young, M. A., & Beveridge, D. L. (1998). Free energy analysis of the conformational preferences of A and B forms of DNA in solution. *Journal of the American Chemical Society*, 120(41),10629–10633. doi:10.1021/ja981307p
- Kaminski, G. A., Friesner, R. A., Tirado-Rives, J., & Jorgensen, W. L. (2001). Evaluation and reparametrization of the OPLS-AA force field for proteins via comparison with accurate quantum chemical calculations on peptides. *The Journal of Physical Chemistry B*, 105(28),6474–6487. doi:10.1021/jp003919d
- Kar, P., Lipowsky, R., & Knecht, V. (2013). Importance of polar solvation and configurational entropy for design of antiretroviral drugs targeting HIV-1 protease. *The Journal of Physical Chemistry B*, 117(19),5793–5805. doi:10.1021/jp3085292
- Kennedy, R. B., Ovsyannikova, I. G., Jacobson, R. M., & Poland, G. A. (2009). The immunology of smallpox vaccines. *Current Opinion in Immunology*, 21(3),314–320. doi:10.1016/j.coi.2009.04.004
- Kennedy, R. B., Poland, G. A., Ovsyannikova, I. G., Oberg, A. L., Asmann, Y. W., Grill, D. E., ... Jacobson, R. M. (2016). Impaired innate, humoral, and cellular immunity despite a take in smallpox vaccine recipients. *Vaccine*, 34(28),3283–3290. doi:10.1016/j.vaccine.2016.05.005
- Kumari, R., Kumar, R., & Lynn, A. (2014). G_mmpbsa: A GROMACS tool for high-throughput MM-PBSA calculations. *Journal of Chemical Information and Modeling*, 54(7),1951–1962. doi:10.1021/ci500020m

- Lee, J., Kumar, S. A., Jhan, Y. Y., & Bishop, C. J. (2018). Engineering DNA vaccines against infectious diseases. *Acta Biomaterialia*, 80,31–47. doi: [10.1016/j.actbio.2018.08.033](https://doi.org/10.1016/j.actbio.2018.08.033)
- Lindler, L. E., Lebeda, F. J., & Korch, G. W. (2004). *Biological weapons defense: Infectious diseases and counter bioterrorism*. New York, NY: Humana Press.
- Lipinski, C. A. (2004). Lead- and drug-like compounds: The rule-of-five revolution. *Drug Discovery Today: Technologies*, 1(4),337–341. doi: [10.1016/j.ddtec.2004.11.007](https://doi.org/10.1016/j.ddtec.2004.11.007)
- Liszewski, M. K., Leung, M. K., Hauhart, R., Buller, R. M. L., Bertram, P., Wang, X., ... Atkinson, J. P. (2006). Structure and regulatory profile of the monkeypox inhibitor of complement: Comparison to homologs in Vaccinia and variola and evidence for dimer formation. *Journal of Immunology*, 176(6),3725–3734. doi:[10.4049/jimmunol.176.6.3725](https://doi.org/10.4049/jimmunol.176.6.3725)
- Luscombe, N. M., Austin, S. E., Berman, H. M., & Thornton, J. M. (2000). An overview of the structures of protein–DNA complexes. *Genome Biology*, 1(1), reviews001. doi:[10.1186/gb-2000-1-1-reviews001](https://doi.org/10.1186/gb-2000-1-1-reviews001)
- Manus, J.-M. (2018). La FDA approuve le premier traitement de la variole arme de guerre. *Revue Francophone Des Laboratoires*, 2018,11. doi: [10.1016/S1773-035X\(18\)30230-2](https://doi.org/10.1016/S1773-035X(18)30230-2)
- Norambuena, T., & Melo, F. (2010). The protein–DNA interface database. *BMC Bioinformatics*, 11,261. doi:[10.1186/1471-2105-11-262](https://doi.org/10.1186/1471-2105-11-262).
- Pittman, P. R., Garman, P. M., Kim, S.-H., Schmader, T. J., Nieding, W. J., Pike, J. G., ... Meyers, M. S. (2015). Smallpox vaccine, ACAM2000: Sites and duration of viral shedding and effect of povidone iodine on scarification site shedding and immune response. *Vaccine*, 33(26),2990–2996. 2015. doi:[10.1016/j.vaccine.2015.04.062](https://doi.org/10.1016/j.vaccine.2015.04.062)
- Prichard, M. N., & Kern, E. R. (2012). Orthopoxvirus targets for the development of new antiviral agents. *Antiviral Research*, 94(2),111–125. doi: [10.1016/j.antiviral.2012.02.012](https://doi.org/10.1016/j.antiviral.2012.02.012). doi:[10.1016/j.antiviral.2012.02.012](https://doi.org/10.1016/j.antiviral.2012.02.012)
- Pronk, S., Páll, S., Schulz, R., Larsson, P., Bjelkmar, P., Apostolov, R., ... Lindahl, E. (2013). GROMACS 4.5: A high-throughput and highly parallel open source molecular simulation toolkit. *Bioinformatics*, 29(7),845–854. doi:[10.1093/bioinformatics/btt055](https://doi.org/10.1093/bioinformatics/btt055)
- Rocha, G. B., Freire, R. O., Simas, A. M., & Stewart, J. J. P. (2006). RM1: A reparameterization of AM1 for H, C, N, O, P, S, F, Cl, Br, and I. *Journal of Computational Chemistry*, 27(10),1101–1111. doi:[10.1002/jcc.20425](https://doi.org/10.1002/jcc.20425)
- Sakhatsky, P., Wang, S., Zhang, C., Chou, T.-H., Kishko, M., & Lu, S. (2008). Immunogenicity and protection efficacy of subunit-based smallpox vaccines using Variola major antigens. *Virology*, 371(1),98–107. doi:[10.1016/j.virol.2007.09.029](https://doi.org/10.1016/j.virol.2007.09.029)
- Shao, Y., Molnar, L. F., Jung, Y., Kussmann, J., Ochsenfeld, C., Brown, S. T., ... Head-Gordon, M. (2006). Advances in methods and algorithms in a modern quantum chemistry program package. *Physical Chemistry Chemical Physics*, 8(27),3172–3319. doi:[10.1039/B517914A](https://doi.org/10.1039/B517914A)
- Silva, A. W. S., & Vranken, W. F. (2012). ACPYPE – AnteChamber Python Parser interface. *BMC Research Notes*, 5,367. doi:[10.1186/1756-0500-5-367](https://doi.org/10.1186/1756-0500-5-367)
- Souza, F. R., Guimarães, A. P., Cuya, T., Freitas, M. P., Gonçalves, A. S., Forgione, P., & França, T. C. C. (2017). Analysis of *Coxiella burnetii* dihydrofolate reductase via *in silico* docking with inhibitors and molecular dynamics simulation. *Journal of Biomolecular Structure and Dynamics*, 35(13),2975–2986. doi:[10.1080/07391102.2016.1239550](https://doi.org/10.1080/07391102.2016.1239550)
- Swain, M. (2012). Chemicalize.org. *Journal of Chemical Information and Modeling*, 52(2),613–615. doi:[10.1021/ci300046g](https://doi.org/10.1021/ci300046g)
- Taylor, C. L., & Junior, L. B. T. (1992). *Chemical and biological warfare*. New York, NY: Franklin Watts.
- Thomsen, R., & Christensen, M. H. (2006). MolDock: A new technique for high- accuracy molecular docking. *Journal of Medicinal Chemistry*, 49(11),3315–3321. doi:[10.1021/jm051197e](https://doi.org/10.1021/jm051197e)
- Trost, L. C., Rose, M. L., Khouri, J., Keilholz, L., Long, J., Godin, S. J., & Foster, S. A. (2015). The efficacy and pharmacokinetics of brincidofovir for the treatment of lethal rabbitpox virus infection: A model of smallpox disease. *Antiviral Research*, 117,115–121. doi:[10.1016/j.antiviral.2015.02.007](https://doi.org/10.1016/j.antiviral.2015.02.007)
- Vorobjev, Y. N., Almagro, J. C., & Hermans, J. (1998). Discrimination between native and intentionally misfolded conformations of proteins: ES/IS, a new method for calculating conformational free energy that uses both dynamics simulations with an explicit solvent and an implicit solvent continuum model. *Proteins: Structure, Function, and Genetics*, 32(4),399–413. doi:[10.1002/\(SICI\)1097-0134\(19980901\)32:4<399::AID-PROT1>3.0.CO;2-C](https://doi.org/10.1002/(SICI)1097-0134(19980901)32:4<399::AID-PROT1>3.0.CO;2-C)
- Wang, C., Greene, D., Xiao, L., Qi, R., & Luo, R. (2018). Recent developments and applications of the MMPBSA method. *Frontiers in Molecular Biosciences*, 4,1–18. doi:[10.3389/fmolb.2017.00087](https://doi.org/10.3389/fmolb.2017.00087).